SOLUTION OF THE PHONON BOLTZMANN TRANSPORT EQUATION EMPLOYING RIGOROUS IMPLEMENTATION OF PHONON CONSERVATION RULES

Tianjiao Wang
School of Mechanical Engineering
Purdue University
585 Purdue Mall
W. Lafayette, IN 47907
wang21@purdue.edu

Jayathi Y. Murthy
School of Mechanical Engineering
Purdue University
585 Purdue Mall
W. Lafayette, IN 47907
jmurthy@ecn.purdue.edu

ABSTRACT

A finite volume scheme is developed to solve the phonon Boltzmann transport equation in an energy form accounting for phonon dispersion and polarization. The physical space and the first Brillouin zone are discretized into finite volumes and the phonon BTE is integrated over them. Second-order accurate differencing schemes are used for the discretization. The scattering term employs a rigorous implementation of phonon momentum and energy conservation laws in determining the rate of normal and Umklapp processes. The method is applied to a variety of bulk silicon and silicon thin-film conduction problems and shown to perform satisfactorily.

NOMENCLATURE

a	Lattice constant, m
A	Amplitude of the wave, m
$\mathbf{b}$	Reciprocal wave vector, 1/m
C_P	Propagating mode specific heat
D	Density of states
e''	Phonon energy density, J/m^3-sr
G	Number of atoms per unit volume
$\mathbf{K}$	Phonon wave vector, 1/m
k	Thermal conductivity, W/mK
k_B	Boltzmann's constant, J/K
M	Atomic mass, kg
N	Phonon distribution function
$\mathbf{r}$	Position vector, m
t	Time, s
T	Temperature, K
v	Speed of sound, m/s
v_g	Group velocity of phonons, m/s
$\hbar$	Reduced Plank's constant, Js
η	Number of polarizations
Ω	Solid angle, sr
τ	Relaxation time, s
ω	Angular frequency of phonons, 1/s
γ	Gruneisen parameter
ρ	Density, kg/m^3
θ	Polar angle, rad
ϕ	Azimuthal angle, rad

INTRODUCTION

In recent years, the aggressive scaling trends of modern microelectronic devices have resulted in increased power dissipation and thermal failures. Accordingly, there has been increasing interest in modeling sub-micron thermal transport in transistors, and therefore in semi-conductors and dielectrics. When the mean free path of phonons is much longer than the domain length scale, Fourier conduction no longer obtains. The phonon Boltzmann transport equation (BTE) has been used to make thermal predictions at the sub-micron scale [1-7]. However, nearly all implementations presented thus far make substantial simplifications, both to the polarization and dispersion behavior of phonons, and to the representation of phonon-phonon scattering. It is unclear what the influence of these approximations is when phonon confinement effects are important or when phonon groups are strongly out of equilibrium with each other, as in modern ultra-scaled MOSFETs.

Among the earliest numerical simulations of the phonon BTE were those published by Majumdar and co-workers [1][2] who employed a discrete ordinates-technique. Frequency-dependence was considered but the scattering terms employed a relaxation time approximation with the frequency-dependent relaxation times being derived to fit bulk thermal conductivity. Ju et al. [3][4] and Sverdrup [5] employed a two-fluid BTE model for heat conduction. The two-fluid model [8] divides phonons into reservoir and propagation modes. The reservoir mode phonons are regarded as capacitive because of their small group velocities, while the propagation mode phonons account for the entire heat transport. The propagation mode employs a single phonon group velocity and a single effective relaxation time is used for energy exchange between reservoir and propagating modes. Under this model, the bulk thermal conductivity is given in terms of the propagating mode

$$k = \frac{1}{3} C_P v_P^2 \tau_P \tag{1}$$

The relaxation time τ_P in [5] is extracted from the bulk thermal conductivity using the heat capacity and group velocity of longitudinal acoustic phonons, which are considered to be in the propagation mode. In contrast, the transverse acoustic and optical phonons are lumped together in the reservoir mode, and

do not contribute to the effective relaxation time. If τ_P is chosen to satisfy bulk thermal conductivity, depending on the choice of the propagating mode velocity, the scattering time for energy transfer between the reservoir and the propagation modes may become very long, and unrealistically high device temperatures would be predicted in typical MOSFETs [6].

The neglect of phonon dispersion effects has significant consequences for the modeling of thermal transport in emerging MOSFETs. It has been pointed out [9] that electron-phonon scattering in MOSFETs transfers energy from electrons preferentially to optical phonons if electron energies are above 60 meV; this energy is then transported to acoustic phonons by scattering between polarizations, and is eventually dissipated to the environment by acoustic phonons. The degree of self-heating in MOSFETs depends critically on which phonon groups receive the energy due to electron-phonon scattering, and how fast this energy can be transported to the environment. Thus, inclusion of phonon dispersion and polarization is critical for capturing the granularity of energy scattering and transport.

To address this issue, Narumanchi et al. [6] proposed a non-gray model, in which phonon dispersion and interactions among longitudinal and transverse acoustic as well as with optical phonons, are accounted for. Expressions for three-phonon interaction times from [10-12], derived from perturbation theory, are used. This non-gray model better captures the underlying physics in the phonon energy transport and has produced good agreements with experimental data in several modeling studies [6][7]. For MOSFET applications, it is capable of capturing the spectrum of relaxation times governing energy exchanges between different phonon groups. However, the scattering terms are approximations modeled on the relaxation time approximation. Furthermore the dispersion curves for silicon in [1,0,0] direction are assumed to hold in all directions. While this approximation is reasonable for bulk silicon, it is not valid for ultra-scaled devices where only in-plane wave vectors have an appreciable density of states. Another issue is phonon energy and momentum conservation rules are not directly satisfied by this model. They are indirectly implied by the relaxation times used, but there is no direct guarantee that only phonons satisfying conservation rules interact. Finally, this model takes its relaxation time expressions from Han and Klemens [12], where a number of approximations about phonon-phonon interactions have been made, many of which are strictly only correct for low temperatures.

Monte Carlo methods have been extensively used in the thermal radiation literature [13]. They also form the basis of electron transport calculations in transistors [14]. Recently, Mazumder and Majumdar [15] has presented a Monte Carlo solution technique for the phonon BTE accounting for phonon dispersion and polarization. In this technique, phonon samples are first drawn from the six individual stochastic spaces, including the three wave vector components and the three position vector components. The samples are then allowed to drift and scatter in time as described by the BTE, and their statistics is collected at various points in time and space, and processed to extract the necessary information. Since the stochastic space is so large, a large number of samples have to be considered in order to obtain sample-independent results. Another important issue is that while relatively simple Monte Carlo schemes can be written for photons and electrons, which are constant in number, the scheme can become very complicated when the number of particles changes, as in the case of phonons. Three-phonon interactions may spawn new phonons or absorb them, and these changes in number must be tracked through appropriate data structures. Furthermore, the approach in [15] finds phonon relaxation times through a curve fit of bulk thermal conductivity, and does not explicitly enforce phonon conservation rules. These complications have, to our knowledge, never been addressed in the phonon transport using Monte Carlo schemes thus far.

The objective of the present work is to substantially improve the modeling of sub-micron heat transfer by considering a rigorous implementation of scattering terms. The energy form of the phonon BTE is used. A general computational procedure for computing three-phonon scattering rates is developed, fully accounting for phonon energy and momentum conservation rules. A finite volume numerical method is developed for the phonon energy density which guarantees exact satisfaction of phonon energy conservation, and which satisfies phonon number and momentum conservation on sufficiently fine discretizations. The scheme is used to compute bulk and thin layer thermal conductivity for silicon and reasonable matches with experimental results are demonstrated. The model presented here paves the way for computing thermal transport in confined geometries with general anisotropic dispersion curves.

THEORY

Phonon Boltzmann Transport Equation

The phonon Boltzmann transport equation (BTE) can be written as [16]

$$\frac{\partial N}{\partial t} + \mathbf{v}_g \cdot \nabla N = \left[\frac{\partial N}{\partial t}\right]_{scatter} \tag{2}$$

Here the phonon number distribution function $N(\mathbf{r},\mathbf{K},t)$ is a function of seven independent variables, time, position and the three components of the wave vector. The scattering term on the RHS includes phonon-phonon, phonon-impurity and phonon-isotope scattering, as well as scattering on other carriers, grain boundaries, imperfections, and sample boundaries.

Three-phonon interactions play a critical role in determining thermal conductivity. There are two types of three-phonon interactions [16]: normal (N) processes, affecting energy transport indirectly by altering the distribution of phonons; and Umklapp (U) processes, posing resistance to energy transport directly by flipping over the direction of the wave vector. The rules governing N and U processes are energy (frequency) and momentum (wave vector) conservation, expressed as

$$\omega + \omega' = \omega'' \qquad \text{(Normal and Umklapp)} \tag{3}$$

$$\mathbf{K}+\mathbf{K}'=\mathbf{K}'' \quad \text{(Normal)}$$
$$\mathbf{K}+\mathbf{K}'=\mathbf{K}''+\mathbf{b} \quad \text{(Umklapp)} \tag{4}$$

where **b** is reciprocal wave vector associated to each given lattice structure. For silicon, there are 14 different **b**'s in the first Brillouin zone [17].

The non-equilibrium phonon distribution function N in Eq. (2) can usually be written as the linear combination of its equilibrium distribution N_0 and a small deviation n from equilibrium

$$N = N_0 + n \tag{5}$$

where N_0 is governed by the Planck or Bose-Einstein distribution [15]

$$N_0 = \frac{1}{\exp(\hbar\omega/k_B T)-1} \tag{6}$$

Assuming an exponential law for the decay process responding to a perturbation, the relaxation time form of the scattering expression can be derived [10]

$$\left[\frac{\partial N}{\partial t}\right]_{scatter} = \frac{N_0 - N}{\tau} = -\frac{n}{\tau} \tag{7}$$

This approximation linearizes the scattering term in the BTE and implies that whenever a system is not in equilibrium, the scattering term will restore the system to equilibrium through an exponential decay N-N_0=exp(-t/τ). The relaxation time approximation essentially limits energy exchanges to a "bath" at N_0 and does not permit direct energy transfers between different groups of phonons.

Energy Form of the BTE

In present work, the energy form of the phonon BTE is preferred since thermal properties and energy transport in silicon are of interest. We define the average phonon energy density as

$$e''(\mathbf{r},\mathbf{K},t) = \int N(\mathbf{r},\mathbf{K},t)\hbar\omega D(\omega)d\omega \Big/ \int D(\omega)d\omega \tag{8}$$

Hence the phonon BTE becomes

$$\frac{\partial e''(\mathbf{r},\mathbf{K},t)}{\partial t} + \mathbf{v}_g(\mathbf{K})\cdot\nabla e''(\mathbf{r},\mathbf{K},t) = \left[\frac{\partial e''(\mathbf{r},\mathbf{K},t)}{\partial t}\right]_{scatter} \tag{9}$$

Here $\mathbf{v}_g(\mathbf{K})$ is the phonon group velocity corresponding to the wave vector **K**. It also varies with the polarization branch, but we do not include this in the notation for simplicity.

Scattering Terms

Three-Phonon Scattering

Based on perturbation theory, Klemens [10][11] derived an expression for scattering rates due to three-phonon interactions

$$\left[\frac{\partial N}{\partial t}\right]_{scatter} = \frac{2\pi\hbar}{M^3}\sum_{\mathbf{K}',\mathbf{K}''}\frac{c^2(\mathbf{K},\mathbf{K}',\mathbf{K}'')}{\omega\omega'\omega''}\delta(\Delta\omega)\delta(\Delta\mathbf{K}) \times\left[(N+1)(N'+1)N''-NN'(N''+1)\right] \tag{10}$$

Here the two delta functions make Eq. (10) become zero unless both energy and momentum conservation rules, Eq. (3) and (4), are satisfied. The coefficient c(**K**,**K**',**K**") may be calculated in terms of anharmonic terms of the potential energy. Instead, Klemens [10] estimated the magnitude of c(**K**,**K**',**K**") in a concise form that has been used in several numerical models and good results have been reported [6][12]. Here,

$$c(\mathbf{K},\mathbf{K}',\mathbf{K}'') = -\frac{i}{\sqrt{G}}\frac{2\gamma M}{\sqrt{3}v}\omega\omega'\omega'' \tag{11}$$

G is the number of atoms per unit volume and v is the speed of sound. We employ this form for simplicity; the procedures required for solving the BTE with alternate forms do not change in the essence.

The terms within the square brackets in Eq. (10) denote the creation/annihilation of phonons in each interaction process. For instance, the term (N+1)(N'+1)N" represents two phonons with distribution functions N and N' which are annihilated to create a third phonon N". Hence the whole terms represent the net rate of creation or annihilation of phonon N. Expanding Eq. (10) using the relations in Eq. (5) and (6) and enforcing energy conservation, Eq. (3), it is possible to show that

$$\left[(N+1)(N'+1)N''-NN'(N''+1)\right] = (nn''+n'n''-nn') + \left[-n(N_0'-N_0'')-n'(N_0-N_0'')+n''(N_0+N_0'+1)\right] \tag{12}$$

When n'= n''=0 and higher order nonlinear terms nn'' etc. are omitted, Eq. (10) recovers the relaxation time approximation.

The summation over all interacting modes **K**' in Eq. (10) can be changed into an integration over the surface S' on which K' is constant, followed by an integration over the interval ΔK' where the direction of **K**' is constant [10]

$$\sum_{\mathbf{K}'} = \eta\frac{V}{(2\pi)^3}\int d\mathbf{K}' = \eta\frac{V}{(2\pi)^3}\int_{K'}dS'\int_{K'}\frac{d\omega'}{v_g} \tag{13}$$

By combining Eq. (10), (11) and (13), and exploiting the property of the delta function

$$\int\delta(x-x')f(x')dx' = f(x) \tag{14}$$

the scattering rate for three-phonon interactions becomes

$$\left[\frac{\partial N}{\partial t}\right]_{scatter} = \eta\frac{\gamma^2\hbar}{3\pi^2\rho v^2}\frac{1}{v_g'}\omega\omega'\omega''\int_{K'}dS' \times\left[(N+1)(N'+1)N''-NN'(N''+1)\right] \tag{15}$$

where ρ=GM/V is the density, η is the number of polarizations of phonon K'.

Impurity Scattering

At low temperatures, for pure single crystals, it is necessary to consider isotope scattering. The isotope scattering rate is taken to be the same as that in Klemens [10]

$$\frac{1}{\tau_I} = \frac{\pi}{6}\Gamma V D(\omega)\omega^2; \quad \Gamma = \sum_i f_i\left[1-\left(M_i/M\right)\right]^2 \tag{16}$$

where M_i is the mass of the impurity atom, M the mass of the host atom, f_i the fractional content of atoms of mass M_i, and the scattering parameter Γ=2.64×10^{-4} for the three silicon isotopes considered. V (=a^3/4) is the volume of a primitive cell.

Boundary Scattering

For the computation of bulk silicon thermal conductivity, boundary scattering is treated in the manner of Holland [18][19]

$$\frac{1}{\tau_B} = \frac{v}{LF} \tag{17}$$

where L is the cross-section size of the sample and F is a factor adjusted to fit experimental data.

These additional scattering mechanisms are included by adding a term of the type

$$\left[\frac{\partial e''}{\partial t}\right]_{scatter} = \frac{e^0 - e''}{\tau} \tag{18}$$

When simulating phonon transport in thin films, boundary scattering is directly computed by resolving specular or diffuse scattering at the domain boundaries.

Computation of Dispersion Curves

Phonon dispersion relations are necessary to correctly model polarization and frequency-dependent behavior and to incorporate the effects of anisotropy in ultra-scaled devices. In present work, the model of Ghatak and Kothari [20], is used to calculate phonon dispersion in bulk silicon.

The equation of motion of atom l in α direction can be written as [20]

$$M\ddot{u}_\alpha(l) = \sum_{l'} F_\alpha(l') \tag{19}$$

where M is the mass, u is the displacement, and F is the forces acting on atom l from all the other atoms l'. The force should be determined directly from interatomic potential, which is usually complicated as in crystal silicon. It is convenient to assume that only central and angular forces, proportional to central and angular displacements, exist between the nearest neighbors [20]. Once a solution of the displacements in the form [20]

$$u_\alpha(l) = A_\alpha \exp[-i(\omega t - \mathbf{K}\cdot\mathbf{r}(l))] \tag{20}$$

is substituted into Eq. (19), the secular determinant is derived from which the dispersion relations can be obtained

$$\left|D_{\alpha\beta}(\mathbf{K}) - \omega^2\delta_{\alpha\beta}\right| = 0 \tag{21}$$

where $\delta_{\alpha\beta}$=1 only if α=β. $D_{\alpha\beta}$ is the dynamical matrix, which is a 6×6 matrix for bulk silicon and given as

$$D_{\alpha\beta}(\mathbf{K}) = \begin{bmatrix} A & 0 & 0 & B & C & D \\ 0 & A & 0 & C & B & E \\ 0 & 0 & A & D & E & B \\ B^* & C^* & D^* & A & 0 & 0 \\ C^* & B^* & E^* & 0 & A & 0 \\ D^* & E^* & B^* & 0 & 0 & A \end{bmatrix} \tag{22}$$

$$A = 4\left(\frac{\alpha_c + 2\alpha_a}{3}\right)$$

$$B = -\left(\frac{\alpha_c + 2\alpha_a}{3}\right)\left(1 + e^{i\frac{(Kx+Ky)}{2}a} + e^{i\frac{(Ky+Kz)}{2}a} + e^{i\frac{(Kz+Kx)}{2}a}\right)$$

$$C = -\left(\frac{\alpha_c - \alpha_a}{3}\right)\left(1 + e^{i\frac{(Kx+Ky)}{2}a} - e^{i\frac{(Ky+Kz)}{2}a} - e^{i\frac{(Kz+Kx)}{2}a}\right) \tag{23}$$

$$D = -\left(\frac{\alpha_c - \alpha_a}{3}\right)\left(1 - e^{i\frac{(Kx+Ky)}{2}a} - e^{i\frac{(Ky+Kz)}{2}a} + e^{i\frac{(Kz+Kx)}{2}a}\right)$$

$$E = -\left(\frac{\alpha_c - \alpha_a}{3}\right)\left(1 - e^{i\frac{(Kx+Ky)}{2}a} + e^{i\frac{(Ky+Kz)}{2}a} - e^{i\frac{(Kz+Kx)}{2}a}\right)$$

where K_x, K_y and K_z are three components of an arbitrary wave vector $\mathbf{K}$, α_c and α_a are central and angular force constants which are determined by fitting to experimentally measured dispersion curves.

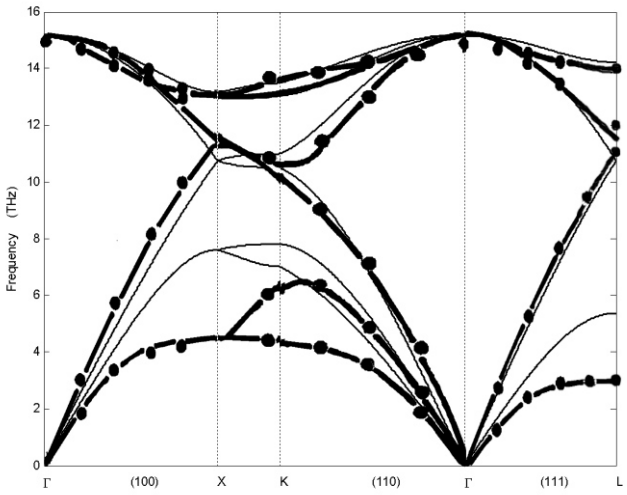

Fig. 1. Phonon dispersion curves for bulk silicon for high symmetry directions. The thin lines are results obtained by present work; the thick lines are obtained by the bond charge model [21], while the solid circles are experimental data [22].

Dispersion curves obtained using [20] are compared with a more accurate bond charge model [21] and experimental data [22] as shown in Fig. 1. Dispersion curves for acoustic phonon branches computed using [20] show discrepancies with respect to experimental data, while for other branches, a good match is obtained. This discrepancy may be ascribed to the simple assumption made in [20] that only central and angular forces exist in bulk silicon. Nevertheless, this lattice dynamics model is still used because it is more convenient to use to compute dispersion for any arbitrary direction

In present work, the dispersion curves in chosen discrete directions are pre-calculated and stored. Phonon properties such as group velocity, specific heat, and density of states are extracted from these directionally-dependent dispersion curves, and eventually incorporated into the proposed full scattering BTE model, as described below.

NUMERICAL SOLUTION

Finite Volume Method

A finite volume method is developed to solve the BTE. The spatial domain is divided into control volumes of volume ΔV. A structured 2D mesh is shown here in Fig. 2 for simplicity, though unstructured implementations of the basic scheme have

been published previously [23]

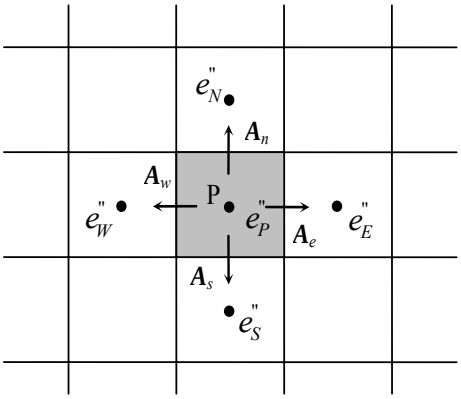

Fig. 2. 2-D spatial domain showing the control volume around point P.

The wave vector space consists of an angular space of extent 4π as well as a wave number space $[0,K_{max}]$, where K_{max} depends on the direction of the wave vector **K**, and captures the non-spherical shape of the first Brillouin zone as shown in Fig. 3.

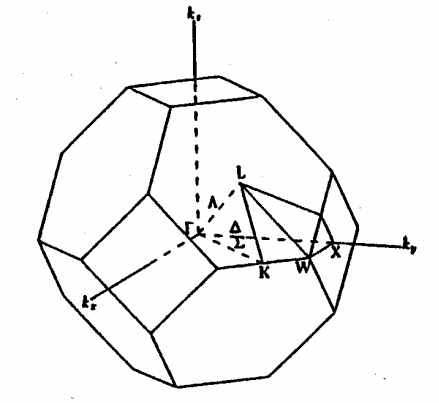

Fig. 3. First Brillouin zone for silicon, Γ-X denotes the [1,0,0] direction, Γ-K the [1,1,1] direction, and Γ-L the [1,1,1] direction.

The angular space is divided into $N_\theta \times N_\phi$ control angles, each of extent $\Delta\Omega_i$. The wave number space is discretized into "bands" of extent ΔK_j. Given a dispersion curve for the polarization under consideration, each band ΔK_j. corresponds to a frequency band $\Delta\omega_j$. We define the direction vector s as

$$\mathbf{s} = \hat{i}\sin\theta\sin\phi + \hat{j}\sin\theta\cos\phi + \hat{k}\cos\theta \tag{24}$$

Here θ and ϕ is polar and azimuthal angle as shown in Fig. 4, respectively.

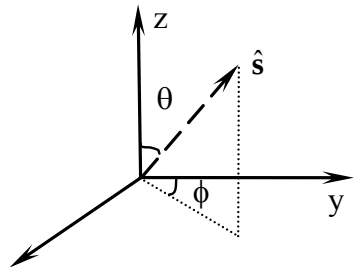

Fig. 4. Polar and azimuthal angles in the direction **s**.

The wave vector is then given by $\mathbf{K}=K\mathbf{s}$ and the phonon velocity vector is given by $\mathbf{v_g}=v_g\mathbf{s}$. Therefore

$$\int D(\omega)d\omega = \int \frac{d^3\mathbf{K}}{(2\pi)^3} = \int\int \frac{K^2 dK d\Omega}{(2\pi)^3} \tag{25}$$

The phonon energy associated with a solid angle $\Delta\Omega_i$ and a band ΔK_i is given by

$$e''_{ij} = \frac{1}{K_j{}^2 \Delta K_j \Delta\Omega_i}\int_{\Delta\Omega_i}\int_{\Delta K_j} N\hbar\omega K^2 dK d\Omega \tag{26}$$

Here $e''_{ij,P}$ is the band and angle-averaged phonon energy density at cell centroid P in the direction i and the frequency band j, and is the solution variable.

For each discrete direction **s**, Eq. (9) is integrated over the solid angle $\Delta\Omega_i$, wave vector band ΔK_j, control volume ΔV_P around point P, and time step Δt to yield [23]

$$(e''_{ij,P} - e''^{n-1}_{ij,P})\frac{\Delta V_P}{\Delta t} + \sum_f |\mathbf{A}_f| J_f v_{ij} e''_{ij,f} = \left[\frac{\partial e''_{ij,P}}{\partial t}\right]_{scatter}\Delta V_P \tag{27}$$

$e''_{ij,f}$ is the average energy density at the face f of the control volume. A simple upwind approximation for $e''_{ij,f}$ can be applied following Patankar [24]. Higher order reconstruction of the face value is also possible [25]. In the results presented here, the smart scheme [24] is used for spatial discretization. A fully implicit scheme is used in Eq. (27). Values at the current time level are un-superscripted in Eq. (27), in contrast to the values at the previous time level, which are superscripted with (n-1). The geometric factor J_f is defined as

$$J_f = \frac{1}{\Delta\Omega_i}\frac{\mathbf{A}_f}{|\mathbf{A}_f|}\cdot\int_{\Delta\theta}\int_{\Delta\phi}\mathbf{s}\sin\theta d\theta d\phi \tag{28}$$

Scattering Term

The relaxation time approximation is not used in present work. The scattering term is written in two parts. The first models elastic scattering processes, i.e., there is no change in the frequency or polarization of the phonon, and the second models three-phonon processes. The scattering term is given by

$$\left[\frac{\partial e''_{ij,P}}{\partial t}\right]_{scatter} = \frac{\left(e^0_{j,P} - e''_{ij,P}\right)}{\tau_{B,ij}} + \frac{\left(e^0_{j,P} - e''_{ij,P}\right)}{\tau_{I,ij}} + \left[\frac{\partial e''_{ij,P}}{\partial t}\right]_{3-phonon} \tag{29}$$

For simplicity, let us consider an interaction of the type $\mathbf{K}+\mathbf{K}'\Leftrightarrow\mathbf{K}''$ in which **K**, **K'** and **K"** satisfy Eqs. (3) and (4). In discrete terms, this involves the interaction of control angle $\Delta\Omega_i$ and the wave number band ΔK_j with ($\Delta\Omega'_k$, $\Delta K'_l$) and ($\Delta\Omega''_m$, $\Delta K''_n$). The three-phonon scattering term for this

interaction may be written as

$$\left[\frac{\partial e''_{ij,P}}{\partial t}\right]_{3-phonon} = \left(\eta \frac{\gamma^2 \hbar}{3\pi^2 \rho v^2} \frac{1}{v_{g,kl}}, \omega_{ij}\omega'_{kl}\omega''_{mn} K_k{}'^2 \Delta\Omega_l{}' \left[(N_{ij,P}+1)(N'_{kl,P}+1)N''_{mn,P} - N_{ij,P}N'_{kl,P}(N''_{mn,P}+1)\right]\right) K_j{}^2 \Delta K_j \Delta\Omega_i \quad (30)$$

where $N_{ij,P}$ is the average phonon number density and is found from the energy density as

$$N_{ij,P} = e''_{ij,P} / \hbar\omega_{ij} \quad (31)$$

Here, ω_{ij} is the centroid value of $\Delta\Omega_i$ and ΔK_j.

In writing Eq. (30), the integral over the surface dS' in Eq. (13) has been approximated by the area of a spherical shell with radius of K', projected by the solid angle $\Delta\Omega$'. Eq. (30) represents only the scattering rate for one single three-phonon interaction process associated with phonon **K**. The total scattering rate is evaluated by summing over all interacting phonons **K'**, as well as by considering interactions of the type $\mathbf{K}+\mathbf{K}'<=>\mathbf{K}''$. Though this discussion has used normal processes as an example, Eq. (30) also applies to Umklapp processes.

Computation of Scattering Interactions

Eq. (30) has been written assuming that the wave vectors **K**, **K'** and **K"** satisfy conservation rules, Eq. (3) and (4). A critical part of the computation procedure is determining *which* phonon interactions satisfy these rules. A general computation procedure has been developed in [26] to find all the possible three-phonon interactions within the first Brillouin zone, with a rigorous enforcement of energy and momentum conservation laws. In this procedure, the first Brillouin zone is discretized into small volumes, each occupied by a group of phonons with the same frequency ω, wave vector **K** and the same polarization. Phonon dispersion relations in each discretized direction are computed based on lattice dynamics, and are used as a known function ω(**K**). For each phonon, a search process thorough all the phonons in the first Brillouin zone is conducted, and all the combinations satisfying conservations rules Eqs. (3) and (4) are recorded as possible three-phonon interactions, each with a scattering rate determined by Eq. (30). Hence a summation over all the interacting phonons **K**' will gives the total scattering rate for a phonon **K**.

Recovery of Temperature

In present work, the lattice "temperature" associated with the total phonon energy is determined by solving the following equation during each iteration

$$\sum_{i,j} e''_{ij} K_j{}^2 \Delta K_j \Delta\Omega_i = \sum_{i,j} e^0_{ij} K_j{}^2 \Delta K_j \Delta\Omega_i \quad (32)$$

where $e_{ij}{}^0$ is the equilibrium phonon energy density associated to phonon solid angle $\Delta\Omega_i$ and band ΔK_j

$$e^0_{ij} = \frac{1}{K_j{}^2 \Delta K_j \Delta\Omega_i} \int_{\Delta\Omega_i} \int_{\Delta K_j} \frac{\hbar\omega}{\exp(\hbar\omega / k_B T) - 1} K^2 dK d\Omega \quad (33)$$

Boundary Conditions

There are three types boundary conditions are admitted in the present model, as described below.

Thermalizing Boundary

These are boundaries at which the phonon energy incoming to the domain from the boundary can be assumed given. For phonons leaving the boundary from the domain, they are regarded as perfectly absorbing boundaries. Thus, the boundary condition is analogous to black boundaries with a given temperature in radiative transfer. For directions incoming to the domain from the domain boundary, the phonon energy density in a frequency band $\Delta\omega_j$ is given by

$$e''_{ij} = e^0_{ij} \quad (34)$$

where e^0_{ij} is defined in Eq. (33).

Symmetrical Boundary

These are boundaries at which the phonon energy in outgoing directions from the boundary is given by

$$e''(\mathbf{s}) = e''(\mathbf{s}_r) \quad (35)$$

where

$$\mathbf{s}_r = \mathbf{s} - 2(\mathbf{s}\cdot\mathbf{n})\mathbf{n} \quad (36)$$

Here **n** is the unit vector normal to the boundary, and is outward-pointing from the domain. A symmetry boundary of this type is only possible if the alignment of the crystal structure with respect to the bounding surface preserves reflective symmetry. In this event, dispersion curves for the **s** and $\mathbf{s}_r$ directions would be the same.

Partially Specular/Partially Diffuse Boundary

These are boundaries at which the phonon energy is reflected partially diffusely and partially specularly. Thus, the phonon energy in a direction **s** entering the domain is determined partially by the corresponding incoming specular direction $\mathbf{s}_r$ and partially by the average over all incoming directions $\mathbf{s}_i$

$$e''(\mathbf{s}) = pe''(\mathbf{s}_r) + (1-p)\sum_{\mathbf{s}_i} e''(\mathbf{s}_i)\left(\int_{\Delta\theta}\int_{\Delta\phi} \mathbf{s}_i \sin\theta d\theta d\phi\right)/\pi \quad (37)$$

Here p is the specularity factor; p=0.0 indicates a completely diffuse boundary, and p=1.0 indicates a completely specular boundary.

RESULTS

Thermal Conductivity of Bulk Silicon

The full scattering BTE model proposed in present work is first validated by computing the thermal conductivity of bulk silicon over a range of temperatures and comparing with experimental data provided in Holland [18][19]. This calculation, though ostensibly simple, constitutes a fundamental test of the scattering model and its implementation. A rectangular domain is considered where the length is chosen so that the lateral acoustic thickness is large enough to ensure that bulk thermal conductivity is independent of domain length. A small temperature difference is maintained between the left and right boundaries, while symmetry boundary conditions are used at the top and bottom boundaries. Boundary scattering is included using Eq. (17) with *L=0.716 cm* and *F=0.8*, as in [18][19]. The BTE is solved with a discretization of 30×3 spatial cells, 4×4 directions in each octant, and 20 divisions in

each wave vector direction. The thermal conductivity is evaluated by computing phonon energy flux across the domain. The plot of the thermal conductivity of bulk silicon over a wide range of temperatures is shown in Fig. 5.

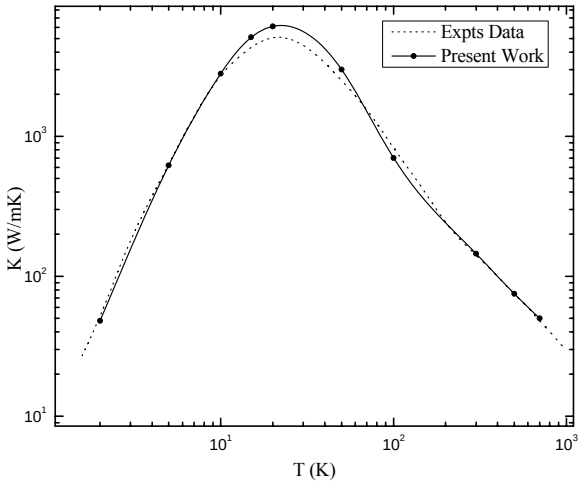

Fig. 5.Thermal conductivity of bulk silicon at different temperatures. Experimental data from Holland [19]

At very low temperatures (<15K), the thermal conductivity of bulk silicon is almost entirely determined by boundary scattering. Good matches with experimental data are obtained even without impurity and three-phonon scattering. This is consistent with our understanding that the number of phonons decreases exponentially with temperature through the Bose-Einstein distribution and three-phonon scattering would be "frozen out" due to the lack of sufficient numbers of phonons at low temperatures.

At higher temperature (>50K), Umklapp processes play the major role in determining thermal conductivity. The match with experimental data for T>50K is good. This match is significant because no fitting with experimental data has been used to determine scattering rates, unlike previous studies [6][12]. The only empirical parameter in the U-process scattering rate is the Gruneisen constant, which is held constant at γ=0.56, consistent with [12]. The match thus establishes the correctness of both the scattering rate expressions as well as the numerical procedure developed here.

In the 20-50K range, N processes play a critical role in enabling U processes to occur. N processes themselves cannot create thermal resistance, and do not directly affect thermal conductivity. However, at low temperatures, there are not sufficient numbers of long **K** phonons, which are necessary for U processes to happen, consistent with Eq. (4). Short **K** phonons must interact in N processes to create long **K** phonons capable of participating in U processes [12].

Thermal Conductivity of Undoped Silicon Film

The full scattering BTE model is next used to compute the in-plane thermal conductivity of undoped silicon thin films. Again, 30×3 spatial cells and 4×4×20 discretization in one octant in wave vector space are used. The top and bottom boundaries are set to be partially diffuse/specular. Various values of the specularity parameter p are tested to best fit the experimental data.

Fig. 6. shows the thermal conductivity of silicon thin films at 300K with thicknesses ranging from *74-850 nm*. The experimental data points are obtained from Ju and Goodson [4] and Asheghi et al [27][28] for comparison. At low temperatures, the plot indicates a better agreement when the specularity factor p is in the range 0.4-0.6.

Fig. 7. shows the thermal conductivity of silicon thin films, with thickness in the range of *0.42-3.0 μm* over a temperature range of *20-300*K. The comparison is with experimental data from Asheghi et al [27][28]. The specularity factor p is set to be *0.4*, compared with the value 0.6 used by Mazumder and Majumdar [15]. This difference may be due to the difference in the scattering model used in the two calculations.

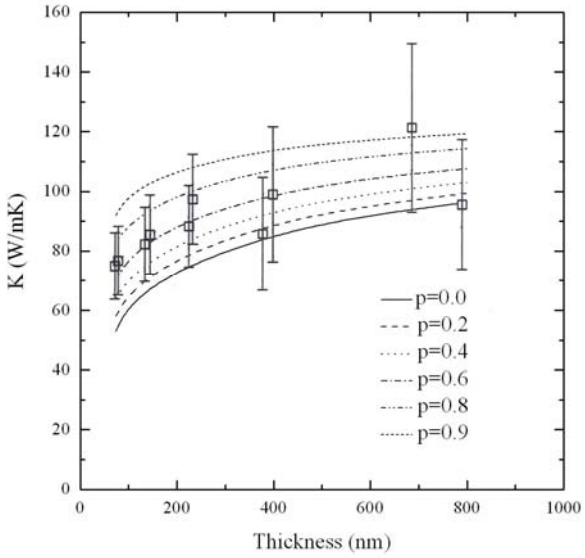

Fig. 6. Thermal conductivity of silicon thin films at 300K for films of different thicknesses. Experimental data from Ju and Goodson [4], and Asheghi et al [27][28]

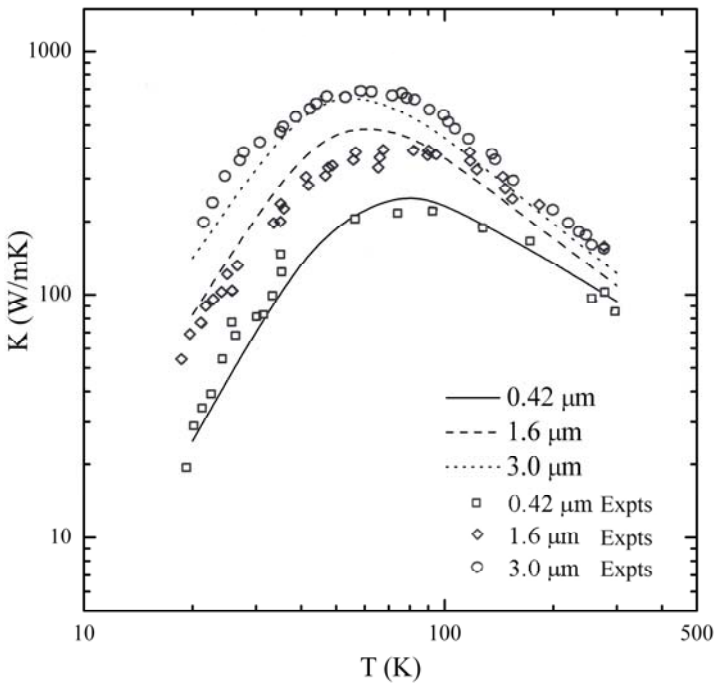

Fig. 7. Thermal conductivity of silicon thin films with p=0.4. Experimental data from Asheghi et al [27][28]

It should be pointed out that in present work, dispersion relations for bulk silicon are used in predicting thin film properties. Though phonon confinement effects have been the focus of much discussion recently [29], the films considered here are much larger than the dominant phonon wavelength at the temperatures of interest and confinement is not expected to play a role here. However, the present implementation is general enough to capture phonon confinement effects in very thin films provided that phase coherence effects are not significant and phonons can still be treated in a particle framework consistent with the Boltzmann transport equation.

SUMMARY AND CONCLUSIONS

A full scattering phonon BTE model has been developed based on the finite volume method. In present model, dispersion and polarization are fully accounted for, and scattering rates are determined by rigorous implementation of phonon conservation rules. The relaxation time approximation is discarded and the full scattering term is incorporated in the BTE. Anisotropy of silicon dispersion curves is also considered so that the realistic shape of the first Brillouin zone is well captured. The model is tested against experimental data for the thermal conductivity of bulk silicon and silicon thin films and a reasonable match with experiments is obtained.

The present model substantially improves the modeling of sub-micron heat transfer in silicon, and allows us to answer fundamental questions about the nature of phonon transport in sub-micron geometries. The role of N and U processes as a function of temperature, the influence of phonon confinement on group velocity and three-phonon scattering rates, and in strongly non-equilibrium heat transfer, such as in micro-electronics, can be answered in the present framework.

ACKNOWLEDGMENTS

Support of J. Murthy and T. Wang under NSF grants EEC-0228390, CTS-0312420 and CTS-0219098 and the Network for Computational Nanotechnology (NCN) is gratefully acknowledged. Support of J. Murthy by the IMPACT Center for Advancement of MEMS/NEMS VLSI, funded by DARPA, through Grant No. HR0011-06-1-0046, under the DARPA N/MEMS Science & Technology Fundamentals Research Program is also acknowledged.

REFERENCES

[1] Majumdar, A., 1993, "Microscale heat conduction in dielectric thin films", ASME J. of Heat Transfer, **115**, pp. 7-16.

[2] Joshi, A.A. and Majumdar, A., 1993, "Transient ballistic and diffusive phonon heat transport in thin films," J. Applied Physics, **74**, No. 1, pp. 31-39.

[3] Ju, Y.S., 1999, "Microscale heat conduction in integrated circuits and their constituent films", Ph.D. thesis, Stanford University.

[4] Ju, Y.S. and Goodson, K.E., 1999, "Phonon scattering in silicon thin films with thickness of order 100 nm", Applied Physics Letters, Vol. 74, No. 20, pp. 3305-3307.

[5] Sverdrup, P.G., 2000, "Simulation and thermometry of sub-continuum heat transport in semiconductor devices", Ph.D. thesis, Stanford University.

[6] Narumanchi, S.V., Murthy, J.Y. and Amon, C.H., 2003, "Computations of sub-micron heat transfer in silicon accounting for phonon dispersion", Proceedings of 2003 ASME Summer Heat Transfer Conference, V 2003, pp. 569-578

[7] Narumanchi, S.V., Murthy, J.Y. and Amon, C.H., 2005, "Comparison of different phonon transport models for predicting heat conduction in silicon-on-insulator transistors", ASME J. of Heat Transfer, Vol. 127, pp. 713-723.

[8] Armstrong, B., 1981, "Two-fluid theory of thermal conductivity of dielectric crystals", Physical Review B, Vol. 23, No. 2, pp. 883–899.

[9] Pop, E., Banerjee, K., Sverdrup, P.G., Dutton, R. and Goodson, K.E., 2001, "Localized heating effects and scaling of sub-0.18 micron CMOS devices", IEEE International Electron Devices Meeting.

[10] Klemens, P.G., 1958, "Thermal conductivity and lattice vibrational modes", in Solid State Physics, edited by Seitz, F. and Thurnbull, D., Vol. 7, pp. 1-98.

[11] Klemens, P.G., 1959, "Theory of the thermal conductivity of solids", in Thermal Conductivity, edited by Tye, R.P., Vol. 1, pp. 1-68.

[12] Han, Y.J. and Klemens, P.G., 1993, "Anharmonic thermal resistivity of dielectric crystals at low temperatures", Physical Review B, Vol. 48, No. 9, pp. 6033-6042.

[13] Modest, M.F., 1993, “Radiative heat transfer”, McGraw-Hill, New York.
[14] Lundstrom, M., 2000, “Fundamentals of carrier transport”, Cambridge University Press, New York.
[15] Mazumder, S. and Majumdar, A., 2001, “Monte Carlo study of phonon transport in solid thin films including dispersion and polarization”, ASME J. of Heat Transfer, **123**, pp. 749-759.
[16] Ziman, J.M., 1960, “Electrons and Phonons”, Oxford University Press, London, United Kingdom
[17] Kittel, C., “Introduction to solid state physics”, 1986, John Wiley & Sons, Inc., New York.
[18] Holland, M.G., 1964, “Phonon scattering in semi-conductors from thermal conductivity studies”, Physical Review, Vol. 134, No. 2A, pp. A471-A480.
[19] Holland, M.G., 1963, “Analysis of lattice thermal conductivity”, Physical Review B, Vol. 132, No. 6, pp. 2461-2471.
[20] Ghatak, A.K. and Kothari, L.S., 1972, “An introduction to lattice dynamics”, Addison-Wesley Publishing, London.
[21] Weber, W., 1977, “Adiabatic bond charge model for the phonons in diamond, Si, Ge, and alpha -Sn”, Physical Review B, Vol. 15, pp. 4789-4803.
[22] Nilsson, G. and Helin, G., 1972, “Study of the Homology between Silicon and Germanium by Thermal-Neutron Spectrometry”, Physical Review B, Vol. 6, pp. 3777-3786.
[23] Murthy, J.Y. and Mathur, S.R., 2002, “Computation of sub-micron thermal transport using an unstructured finite volume method”, ASME Journal of Heat Transfer, Vol. 124, pp. 1176-1181.
[24] Patankar, S.V., 1980, “Numerical Heat Transfer and Fluid Flow”, McGraw-Hill, New York.
[25] Mathur, S.R. and Murthy, J.Y., 1997, “A pressure based method for unstructured meshes”, Numerical Heat Transfer Part B, Vol. 31, No. 2, pp. 195-216.
[26] Wang, T. and Murthy, J.Y., 2004, “An improved computation procedure for phonon relaxation times”, Proceedings of IMECE2004, IMECE2004-61901.
[27] Asheghi, M., Touzelbaev, M.N., Goodson, K.E., Leung, Y.K., and Wong, S.S., 1998, “Temperature-dependent thermal conductivity of single-crystal silicon layers in SOI substrates”, J. of Heat Transfer, **120**, pp. 30-36.
[28] Asheghi, M., Kurabayashi, K., Kasnavi, R., and Goodson, K.E., 2002, “Thermal conduction in doped single-crystal silicon films”, J. of Applied Physics, 91, No. 8, pp. 5079-5088.
[29] Yang, B. and Chen, G., 2000, “Lattice dynamics study of phonon heat conduction in quantum wells”, Phys. Low-Dim. Struct., 5/6, pp. 37-48